Testing Specific Theories Beyond General Relativity with LIGO

Natalie Malagon, Mentor: Ethan Payne

August 7, 2023

Abstract

Gravitational waves observed by LIGO allow us to test general relativity in the strong-field regime with populations of binary merger events. Observations thus far are consistent with general relativity at both the individual and population level. Current tests of general relativity utilize a single deviation parameter rather than generic deviation parameters, which makes it difficult to map this information to specific theories and robustly test them over ensembles of events. We apply Bayesian inference to the inspiral phase of gravitational-wave signals in binary black hole merger events, to obtain posterior distributions for the 15 source parameters and 10 post-Newtonian deviation parameters. This parameter estimation involves the hybrid sampling method which uses nested sampling to seed parallel-tempered Markov Chain Monte Carlo (MCMC) ensembles and allows us to explore degenerate parameter spaces. We apply a Principal Component Analysis (PCA) to reduce the dimensionality of the parameter space, to understand the underlying correlations between the deviation parameters. Hierarchical inference could then be applied to ensembles of events to test specific theories beyond general relativity, such as the dynamical Chern Simons (dCS) and Einstein-dilaton Gauss-Bonnet (EdGB) theories. This would result in constraining the bounds on the coupling coefficients that characterize these specific theories.

1 Introduction

The Laser Interferometer Gravitational-Wave Observatory (LIGO) has opened up a new era of physics with its first observation of a binary black hole merger [1]. Approximately 90 compact binary merger events have been observed thus far with the latest gravitational-wave transient catalog (GWTC-3) [2]. LIGO utilizes dual recycled, Fabry-Pérot-Michelson interferometers to measure gravitational-wave emissions from distant astrophysical sources [3]. Binary black hole mergers are characterized by two orbiting black holes that undergo distinct phases: an inspiral, merger, and ringdown phase that results in the formation of a single massive black hole [4]. Once the black holes form a binary system, through the emission of gravitational waves, the binary black holes lose orbital angular momentum and eccentricity which leads the black holes to inspiral in a quasi-circular orbit. As the orbiting black holes approach the merger, numerical relativity methods characterize this stage because the post-Newtonian expansion that describes the inspiral loses accuracy [5]. At the start of the merger, there is a plunge where the black hole horizons merge as their orbits become unstable. The resulting remnant black hole becomes stable in the ringdown stage and its gravitational-wave radiation is characterized by quasi-normal modes [6]. The gravitational-wave radiation provides the opportunity to test fundamental physics in the strong-field, highly dynamical regime of gravity which has been previously inaccessible in experimental tests of general relativity [7].

With the current population of binary merger events detected by LIGO, there has been consistency with predictions of general relativity in the strong-field regime [8–10]. By assuming general relativity is accurate, we are able to place constraints on alternative theories [11]. Einstein's general theory of relativity has been tested extensively in the weak-field regime, yet theoretical expectations suggest that at high energies general relativity breaks down [12]. This motivates testing theories around compact sources such as binary black hole mergers which involve stronger curvatures and shorter dynamical time scales [3, 12].

During the inspiral phase, gravitational-wave signals transition from weak fields to moderately strong fields, and spacetime is violently curved when binaries merge [13]. The inspiral phase can be accurately

modeled with a post-Newtonian formalism [5]. The post-Newtonian formalism is a method for solving Einstein's field equations in the weak-field regime and it has been proven to be effective in describing fast, strong-field systems [14]. This method perturbatively expands the binary's evolution in powers of orbital frequency. Post-Newtonian phasing coefficients describe the physical effects in the relativistic dynamics of binaries, such as spin-spin interactions [15]. By focusing on the inspiral phase, we aim to look for potential deviations from general relativity.

As LIGO becomes more sensitive, the number of binary mergers will grow which will allow for deviations to be more accurately constrained. By analyzing inspiral phase post-Newtonian coefficients for many gravitational-wave events, we are able to understand alternate theories whose coefficients vary in their post-Newtonian expression. The consistency of these coefficients with predictions of general relativity serve as a precise, independent test of the theory [10, 15].

In Section 2, we describe the hybrid sampling method and hierarchical inference. In Section 3 we apply the hybrid sampling method to simulated gravitational-wave signals and demonstrate that it shows correlations between deviation parameters. Challenges and implications are discussed in Section 4.

2 Methodology

2.1 Hybrid Sampling

The first objective involves applying hybrid sampling via Bilby to jointly infer the 15 source, general relativity, parameters of the binary black hole merger events in GWTC-3 and 10 post-Newtonian deviation parameters [16]. The hybrid sampling method is computationally efficient and recovers posterior distributions [10]. This method treats general relativity as the initial prediction in order to initialize the deviation parameter estimation. For each gravitational-wave signal, the data is sampled first using nested sampling via dynesty [17]. These nested samples initialize the walkers of a parallel tempered Markov Chain Monte Carlo (MCMC) with the implementation of the package ptemcee in order to obtain generic, multi-dimensional samples [18, 19].

2.2 Hierarchical Inference

After generating posterior distributions for all the astrophysical and deviation parameters, we will apply a hierarchical approach to test specific theories using all the possible deviations from general relativity for each gravitational-wave event. This hierarchical procedure involves combining multiple gravitational wave events and marginalizing over individual event parameters [9]. In sampling the parameters of these events, we are able to understand the underlying population parameters. These population parameters can describe the coupling coefficients of specific theories beyond general relativity. The hierarchical inference method further entails using a Gaussian Mixture Model (GMM), which is a computationally inexpensive density estimation procedure [20]. The GMM estimates the posterior probability densities of each individual event. This is accomplished by efficiently evaluating the likelihood functions for each event [9].

3 Results

For our source model, the post-Newtonian parameterization of the phase evolution during the inspiral phase of the general relativistic waveform in the frequency domain is

$$\Phi(f) = 2\pi f t_c - \phi_c - \frac{\pi}{4} + \frac{3}{128} \times \sum_{k=0}^{7} \frac{1}{\eta^{k/5}} \Big(\varphi_k + \varphi_{k,l} \ln f\Big) f^{(k-5)/3} \,,$$

where t_c is the time and ϕ_c is the phase when the binary black holes coalesce, $\eta \equiv \frac{m_1 m_2}{M^2}$ is the symmetric mass ratio of the system, and f is the frequency [21].

We have started running the hybrid sampling method, focusing on the inspiral phase of a simulated binary black hole signal. This injection only has a modification of 20% to the φ_2 parameter, first order post-Newtonian term, in order to test if deviations could be recovered from this method. In this hybrid sampling

step, the initial deviation parameter walkers are Gaussian distributed. In addition, there is a greater than 0.9 match cut to the general relativity waveform. In this assumption, we restrict the deviation to be within 10% of the waveform which is indicative that the waveform appears to be similar to the general relativity waveform.

We have completed two parameter estimation runs on the injected signal with the hybrid sampling method. In this first run, all the deviation parameters were modified separately, similar to [10]. Meanwhile, on the second run, we have changed all the deviation parameters simultaneously. By changing each of the deviation parameters, they are then able to be generalized in order to extend them to specific theories. Figure 1 shows the posterior distributions for a few deviation parameters. In directly plotting the two-dimensional representation of parameters, we can search for correlations between them through visual inspection. In particular, correlations between deviation parameters can reflect how near-identical waveforms can be generated using different parameters.

The corner plot in Figure 1 denotes the marginal posterior distributions and their two-dimensional posterior distributions. Given that the posterior distributions are roughly smooth, this indicates that the parameters successfully converged using the hybrid sampling method, even when the deviation parameters are jointly inferred. There is a positive correlation between the chirp mass, $\mathcal{M}$, and the deviation parameter, $\delta\varphi_1$. This can be indicative of the relationship between the two parameters in Eq. 1. In Figure 1, there also appears to be a correlation between $\delta\varphi_2$ and $\delta\varphi_3$. It can be reasonably inferred that this is due to these parameters describing the early inspiral regime.

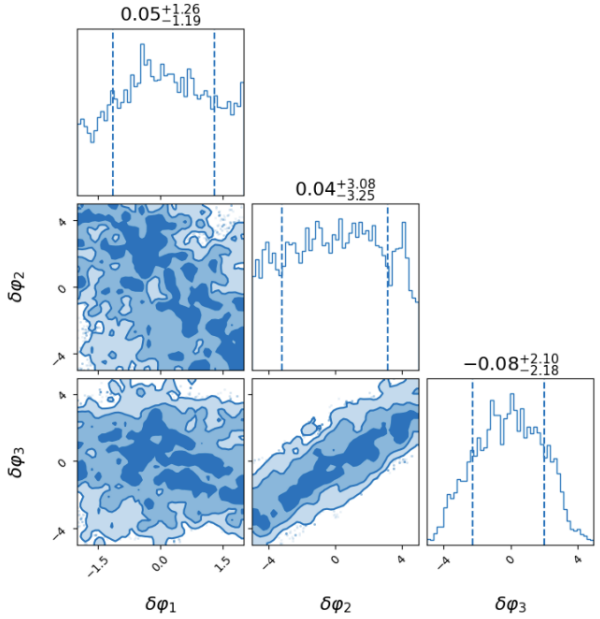

Figure 1: Marginal posterior distributions of three deviation parameters resulting from jointly inferring each deviation parameter.

To improve this posterior distribution, signal-to-noise ratio (SNR) and overlap cuts were applied to produce 10 injection parameters that more closely align with real gravitational wave signals and do not significantly deviate from general relativity. Injections were randomly sampled until SNR > 20, to ensure the gravitational wave signals were not buried by the detector's noise. These injections were narrowed down further by having the SNR be less than the frequency of their innermost stable circular orbit,

$$f_{ISCO} = \frac{c^3}{6\sqrt{6}G(m_1 + m_2)}\,, \tag{1}$$

where m_1 and m_2 are the component masses. In this context, the innermost stable circular orbit is the moment before the binary black hole merges and this cut allows us to capture the inspiral phase.

The overlap $O > 0.9$,

$$O = |\frac{\langle \tilde{h}_{GR}, \tilde{h}_{BGR} \rangle}{\sqrt{\langle \tilde{h}_{GR}, \tilde{h}_{GR} \rangle \langle \tilde{h}_{BGR}, \tilde{h}_{BGR} \rangle}}| \tag{2}$$

was derived where $\tilde{h}_{GR}$ is the +-polarization of the general relativity waveform in the frequency domain and $\tilde{h}_{BGR}$ is the +-polarization of the beyond general relativity waveform [10]. The inner products between the waveforms are weighted with the power spectral density from the detector, where there is no instantiated noise. The same source parameters were used in $\tilde{h}_{GR}$ and $\tilde{h}_{BGR}$. As seen in Figure 2, the waveforms in the time domain with these cuts appear to resemble real gravitational wave signals. In this example, the beyond general relativity waveform had a deviation in $\delta\varphi_2$.

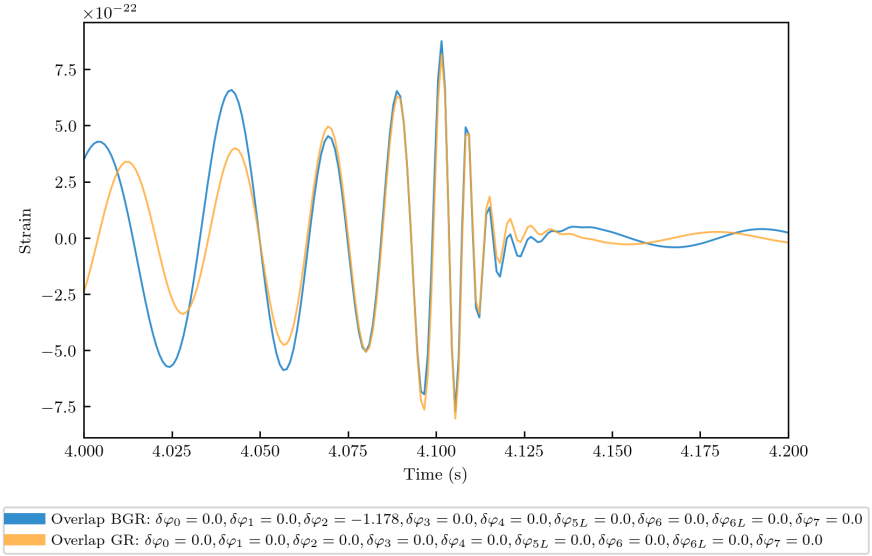

Figure 2: Beyond general relativity strain in the time domain for an injection that includes the SNR and overlap cuts and its associated general relativity waveform.

Another parameter estimation run was made with these cuts and adjusted parallel-tempered MCMC parameters. The number of steps used by ptemcee increased to 200 and the unburnt chains were stored in the result. Figure 3 shows the improved marginal and joint distributions for an example of injection parameters. The same correlation between $\delta\varphi_2$ and $\delta\varphi_3$ is seen, and the marginal distributions for each of the displayed parameters have converged towards their true parameters except $\delta\varphi_4$ which has converged to a roughly uniform distribution. The likelihoods were evaluated to try to understand the posterior distribution of $\delta\varphi_4$. The likelihoods were calculated given the source parameters that correspond to a particular likelihood value, such as the maximum likelihood value, along the $\delta\varphi_4$ prior range. In Figure 4 the parameters from the maximum, minimum, and two randomly sampled likelihood values were used to calculate their likelihoods. The resulting likelihood distributions appear Gaussian which indicates that there are potentially underlying correlations in the marginal posterior distributions that are not being seen. In the future, a Principal Component Analysis (PCA) will be applied to reduce the dimensionality and better understand the parameter space [22]. By obtaining the eigenvalues and eigenvectors in the PCA decomposition, we will be able to understand the degeneracies involved because the eigenvectors that correspond to the variance-covariance matrix will provide new parameters where the accurate likelihoods can be represented [23].

4 Conclusions

A challenge that we encountered included trying to improve past results, such as Figure 1, and determining whether the lack of convergence in the marginal distributions for certain parameters was due to the sampler or

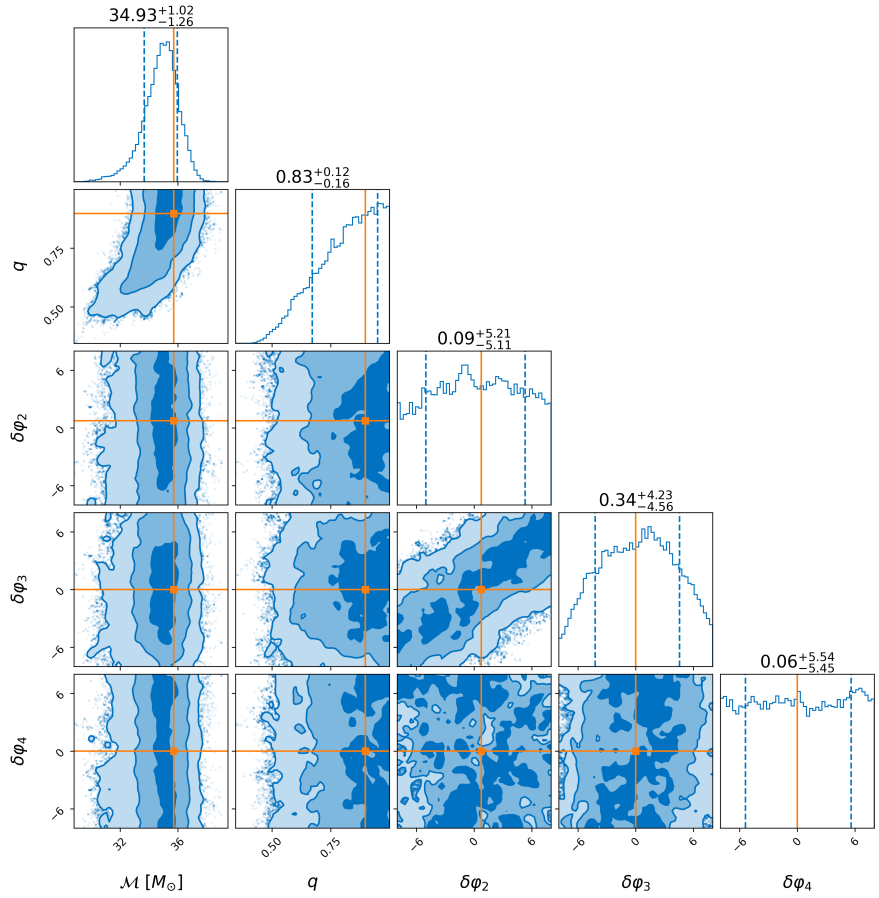

Figure 3: Marginal posterior distributions of the $\mathcal{M}$, q, and deviation parameters resulting from the SNR and overlap cuts and improved ptemcee parameters.

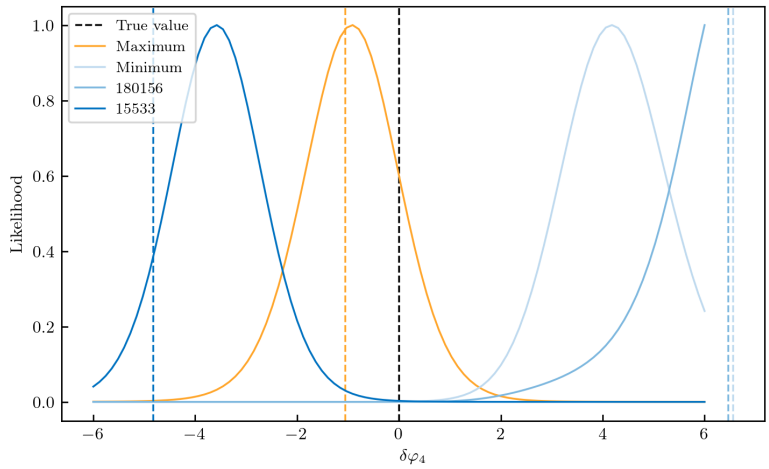

Figure 4: Likelihood over a range of $\delta\varphi_4$ values.

injection parameters. In trying to assess whether there was an issue with the sampling method or waveform, we checked the convergence of the posterior distributions with cuts to the injection samples, visualized the injection waveforms, and evaluated likelihoods across deviation parameters. From comparing visualizations

of the waveforms of injections with or without the SNR and overlap cuts, it was evidently necessary that only injection parameters that resulted from the cuts should be used. A subsequent parameter estimation run was made where these cuts and slightly modified parallel-tempered MCMC sampling parameters were used, as described in Section 3. Though the marginal posterior distributions improved, the likelihoods over a variety of $\delta\varphi_4$ values revealed a Gaussian likelihood surface. This motivates our next step in applying PCA to better disentangle the correlations between the deviation parameters and obtain improved posterior distributions for the set of deviation parameters.

References

[1] B. P. Abbott et al. LIGO: The Laser interferometer gravitational-wave observatory. *Rept. Prog. Phys.*, 72:076901, 2009.

[2] R. Abbott et al. GWTC-3: Compact Binary Coalescences Observed by LIGO and Virgo During the Second Part of the Third Observing Run. 11 2021.

[3] B. P. Abbott et al. Tests of general relativity with GW150914. *Phys. Rev. Lett.*, 116(22):221101, 2016. [Erratum: Phys.Rev.Lett. 121, 129902 (2018)].

[4] Jeroen Meidam et al. Parametrized tests of the strong-field dynamics of general relativity using gravitational wave signals from coalescing binary black holes: Fast likelihood calculations and sensitivity of the method. *Phys. Rev. D*, 97(4):044033, 2018.

[5] Luc Blanchet. Gravitational Radiation from Post-Newtonian Sources and Inspiralling Compact Binaries. *Living Reviews in Relativity*, 17(1):2, December 2014.

[6] R. Abbott et al. Tests of general relativity with binary black holes from the second LIGO-Virgo gravitational-wave transient catalog. *Phys. Rev. D*, 103(12):122002, 2021.

[7] Harsh Narola, Soumen Roy, and Anand S. Sengupta. Beyond general relativity: Designing a template-based search for exotic gravitational wave signals. *PhRvD*, 107(2):024017, January 2023.

[8] B. P. Abbott et al. Tests of General Relativity with the Binary Black Hole Signals from the LIGO-Virgo Catalog GWTC-1. *Phys. Rev. D*, 100(10):104036, 2019.

[9] Jacob Golomb and Colm Talbot. Hierarchical Inference of Binary Neutron Star Mass Distribution and Equation of State with Gravitational Waves. *ApJ*, 926(1):79, February 2022.

[10] Noah E. Wolfe, Colm Talbot, and Jacob Golomb. Accelerating tests of general relativity with gravitational-wave signals using hybrid sampling. *Phys. Rev. D*, 107(10):104056, 2023.

[11] R. Abbott et al. Tests of General Relativity with GWTC-3. 12 2021.

[12] Emanuele Berti et al. Testing General Relativity with Present and Future Astrophysical Observations. *Class. Quant. Grav.*, 32:243001, 2015.

[13] Kent Yagi, Leo C. Stein, Nicolás Yunes, and Takahiro Tanaka. Erratum: Post-Newtonian, quasicircular binary inspirals in quadratic modified gravity [Phys. Rev. D 85, 064022 (2012)]. *PhRvD*, 93(2):029902, January 2016.

[14] Clifford M. Will. Inaugural Article: On the unreasonable effectiveness of the post-Newtonian approximation in gravitational physics. *Proceedings of the National Academy of Science*, 108(15):5938–5945, April 2011.

[15] M. Saleem, Sayantani Datta, K. G. Arun, and B. S. Sathyaprakash. Parametrized tests of post-Newtonian theory using principal component analysis. *PhRvD*, 105(8):084062, April 2022.

[16] Gregory Ashton et al. BILBY: A user-friendly Bayesian inference library for gravitational-wave astronomy. *Astrophys. J. Suppl.*, 241(2):27, 2019.

[17] Joshua S. Speagle. DYNESTY: a dynamic nested sampling package for estimating Bayesian posteriors and evidences. *MNRAS*, 493(3):3132–3158, April 2020.

[18] Daniel Foreman-Mackey, David W. Hogg, Dustin Lang, and Jonathan Goodman. emcee: The MCMC Hammer. *PASP*, 125(925):306, March 2013.

[19] W. D. Vousden, W. M. Farr, and I. Mandel. Dynamic temperature selection for parallel tempering in Markov chain Monte Carlo simulations. *MNRAS*, 455(2):1919–1937, January 2016.

[20] Colm Talbot and Eric Thrane. Flexible and Accurate Evaluation of Gravitational-wave Malmquist Bias with Machine Learning. *ApJ*, 927(1):76, March 2022.

[21] Dimitrios Psaltis, Colm Talbot, Ethan Payne, and Ilya Mandel. Probing the black hole metric: Black hole shadows and binary black-hole inspirals. *PhRvD*, 103(10):104036, May 2021.

[22] Muhammed Saleem, Sayantani Datta, K. G. Arun, and B. S. Sathyaprakash. Parametrized tests of post-Newtonian theory using principal component analysis. *Phys. Rev. D*, 105(8):084062, 2022.

[23] Sayantani Datta, M. Saleem, K. G. Arun, and B. S. Sathyaprakash. Multiparameter tests of general relativity using principal component analysis with next-generation gravitational wave detectors. 8 2022.